

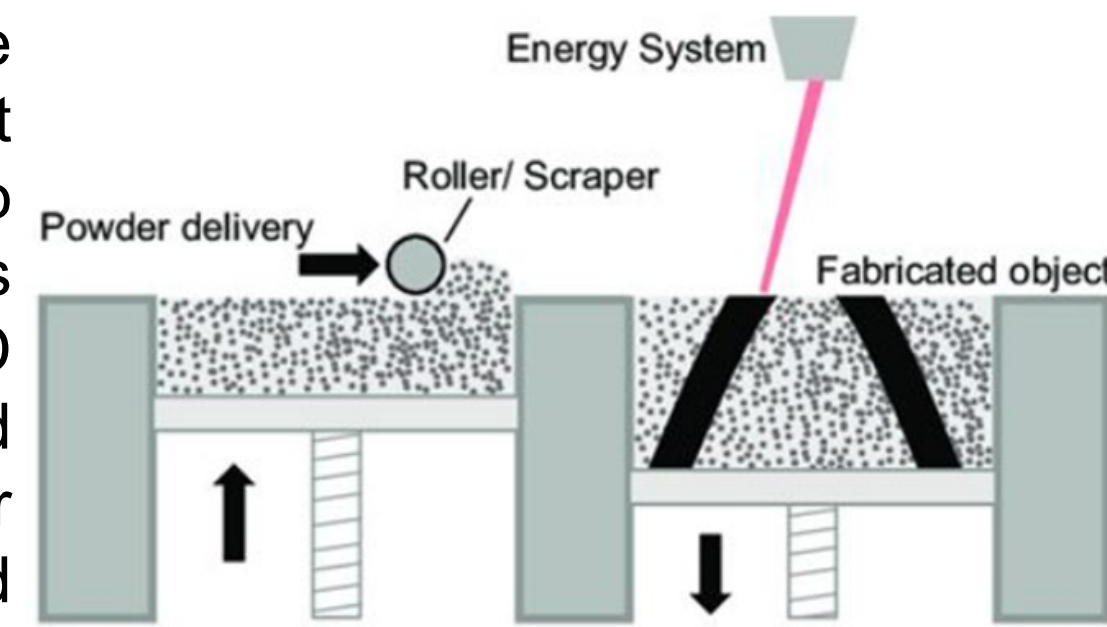
**Abstract:** Mar-M509 cobalt alloys have various high temperature applications for the aerospace industry. In this project, Mar-M509 alloys were produced by laser powder bed fusion (LPBF). Oxides were introduced to investigate the influence of oxide particles on microstructure and mechanical properties. SEM and EDS demonstrate that oxide particles tend to agglomerate within the sample causing crack initiation. X-ray diffraction (XRD) shows the evolution of texture as a result of the introduction of oxides. Microhardness and tensile properties of the alloys were investigated, and oxide inclusions appeared to lower tensile strengths and microhardness.

This work is sponsored by Praxair Surface Technologies Inc  
 A Linde company



## Background

Laser powder bed fusion (LPBF) is an additive manufacturing technique that uses a high-power laser to melt layers of metal powders to form complex 3D geometries. Alloys produced via LPBF are known for their exceptional strength and fatigue lives at high temperatures, and are often used in high stress, high temperature applications such as gas turbine blades. Compared to traditional casting methods, LPBF can produce parts with high levels of detail, with retained strength and ductility due rapid solidification rates.

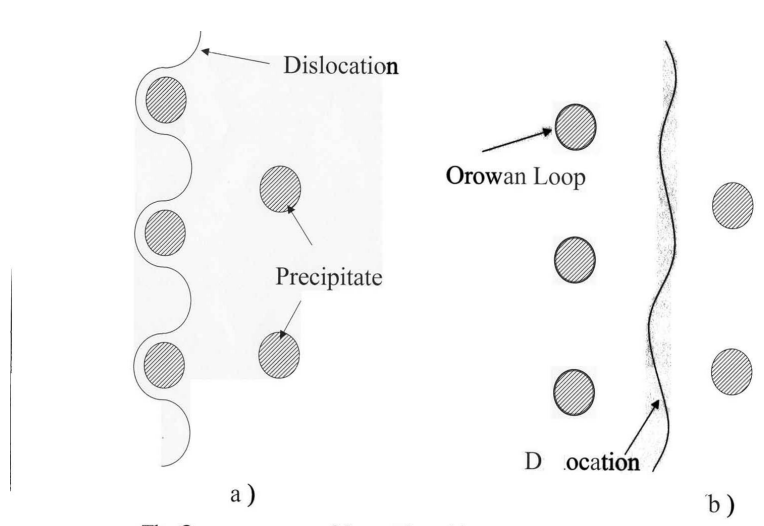


Mar-M509 is a cobalt-based alloy that may be used as a replacement for nickel-based alloys common in gas turbine engines due to the extreme thermal and fluid aero environment. The unique carbide and cellular structure of Mar-M509 create stable intermetallic phases that lead to Mar-M509's superior high temperature creep and corrosion resistance.

### Weight Percent Composition of Mar-M509 powder powder

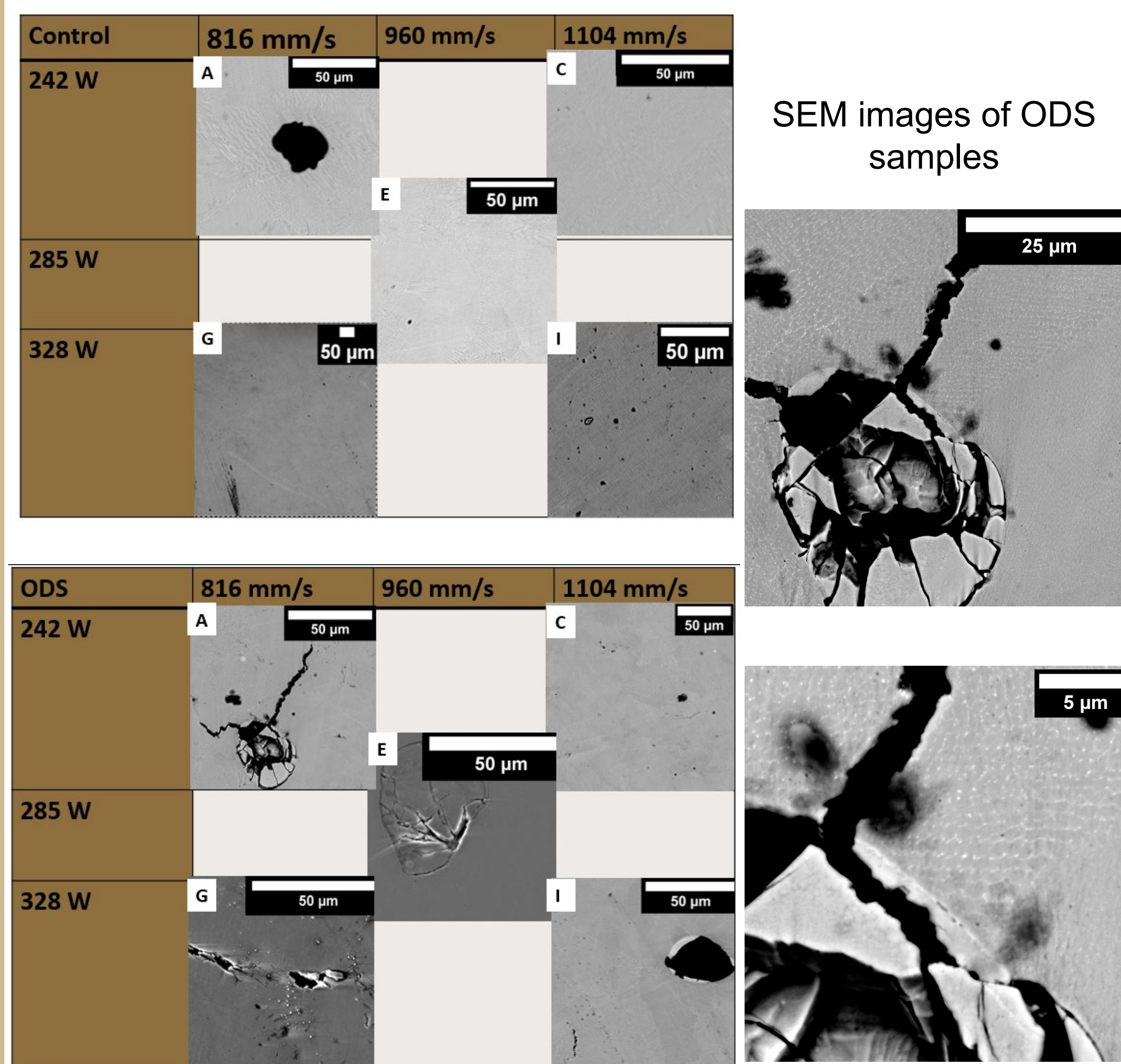
Co	Cr	Ni	W	Ta	C	Zr	Si	Ti	Fe	Trace
Bal	23.65	10.12	7.33	3.41	0.6	0.4	0.26	0.23	0.04	0.18

Oxides will be added into the MAR-M509 powder in attempt to create oxide dispersion strengthening (ODS) via Orowan looping. We hypothesize that dislocations bowing around oxide additives will decrease the stress on the lattice and increase the materials yield strength



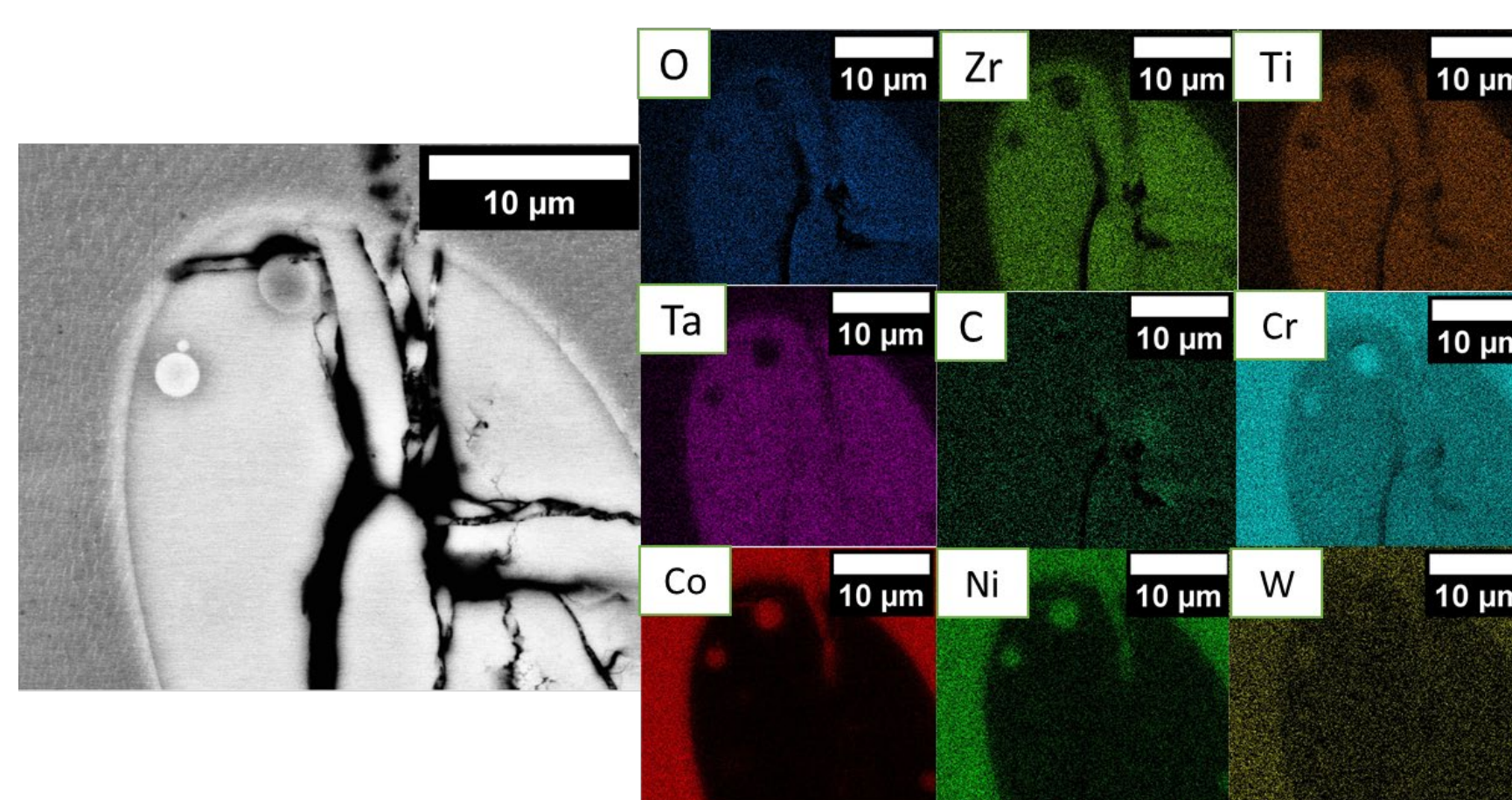
## Microstructure Analysis

### SEM



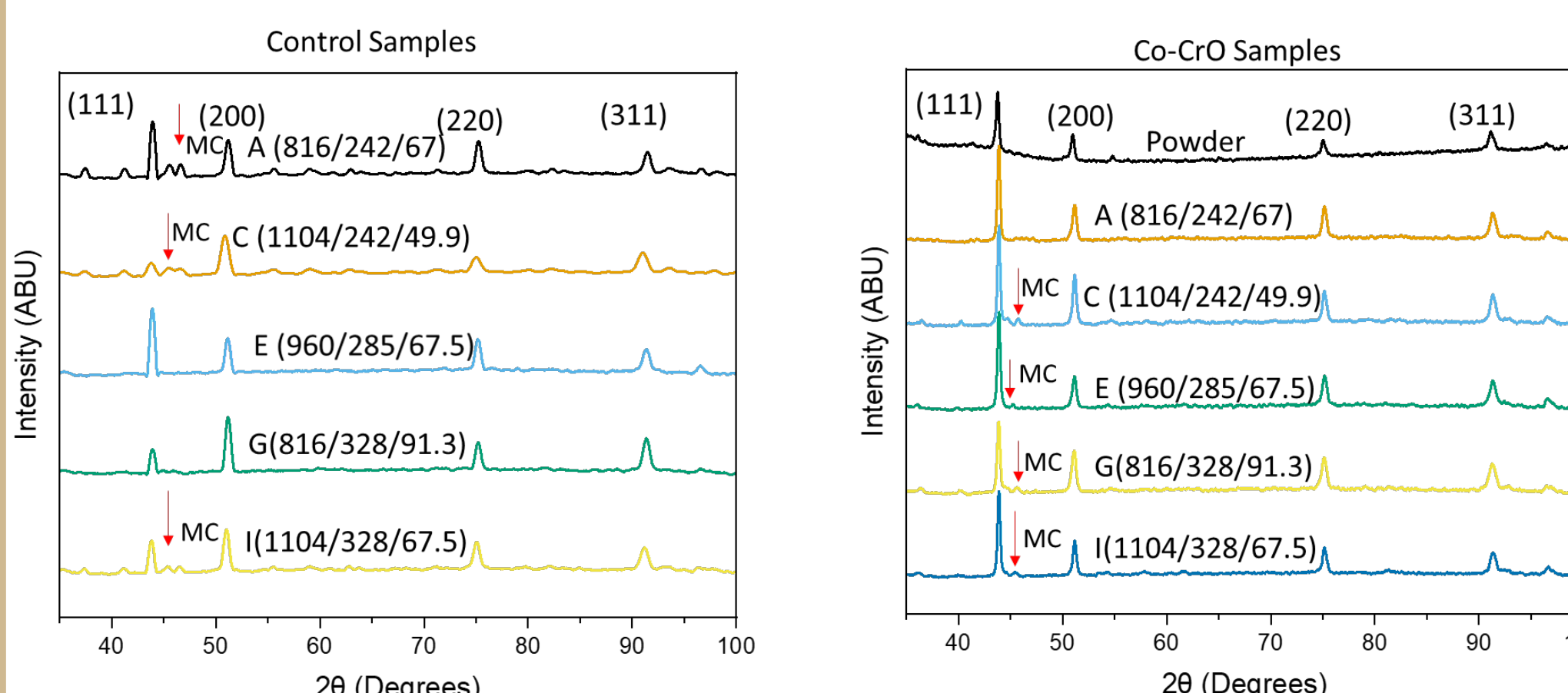
Compared to the control, the ODS Mar-M509 Cobalt Alloy demonstrated a relatively high degree of agglomeration and cracking for most printing parameters. The cracks often originated from ~40µm spherical particles near cobalt grain boundaries. The size of the particles and the nature of the cracks are both indicators of agglomeration of the oxide dispersant causing crack initiation in the ODS samples. Cracking may occur due to Coefficient of Thermal Expansion mismatch between oxide agglomerates and cobalt matrix increasing stress on the lattice.

### EDS



EDS analysis reported excess oxygen, aluminum, titanium, zirconium, and tantalum within the agglomerate particle, pointing towards diffusion of these elements into the oxide followed by oxidation of elements in the matrix. This supports the conclusion that the particles seen in EDS are oxide agglomerates

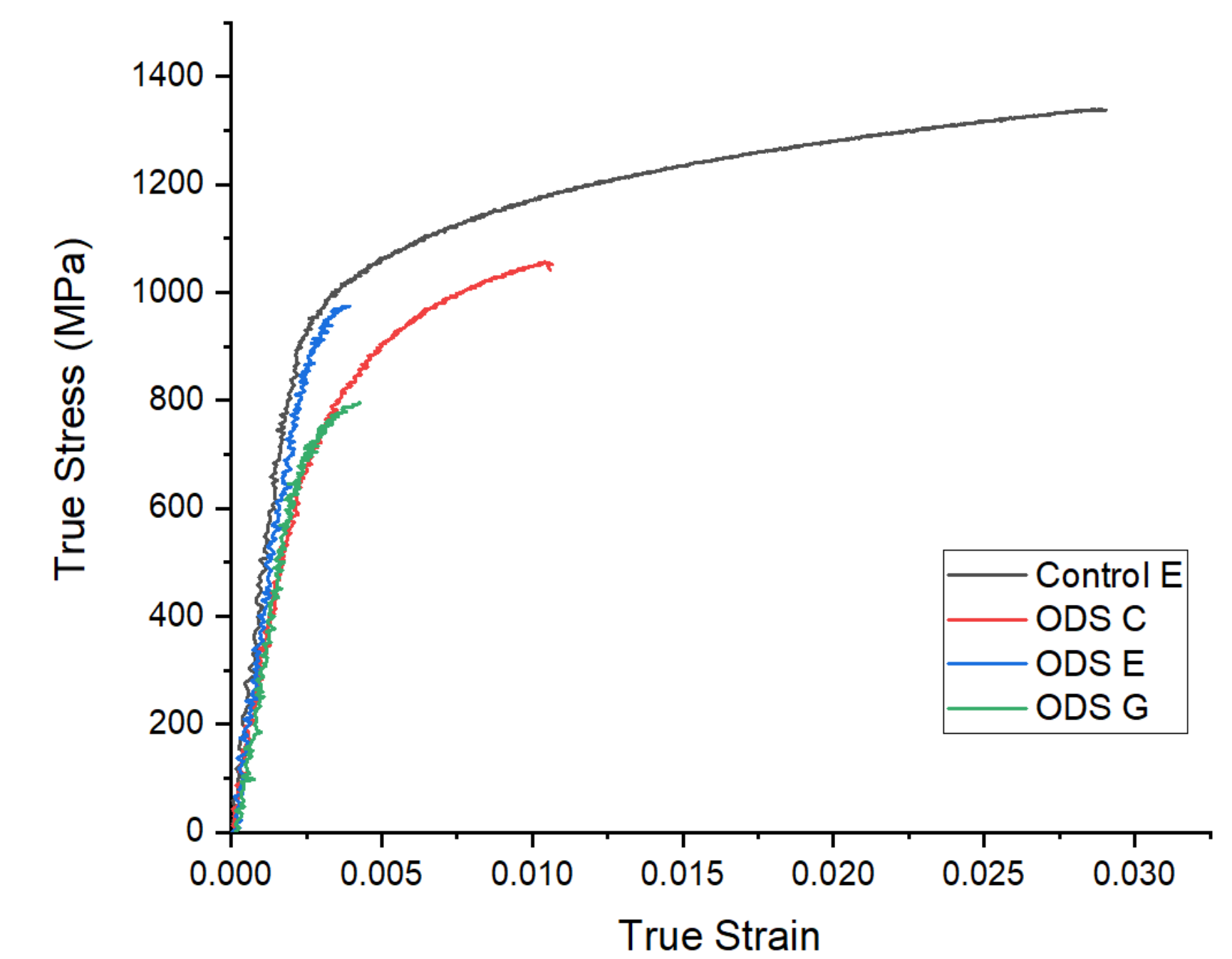
### XRD



XRD patterns were taken from the XY plane of the samples. The data labels correspond to (laser power (W), laser scan speed (mm/s) and energy density (J/mm³)). Co-CrO samples have a dominant (111) peak while the dominant peak varies from (111) and (200) depending on laser parameters in the control samples. All samples except sample A have identifiable metal carbide (MC) peaks around 46°, while samples A, C, and I have the same identifiable MC peaks. The addition of CrO could have potentially removed some texture from the Mar-M509 samples.

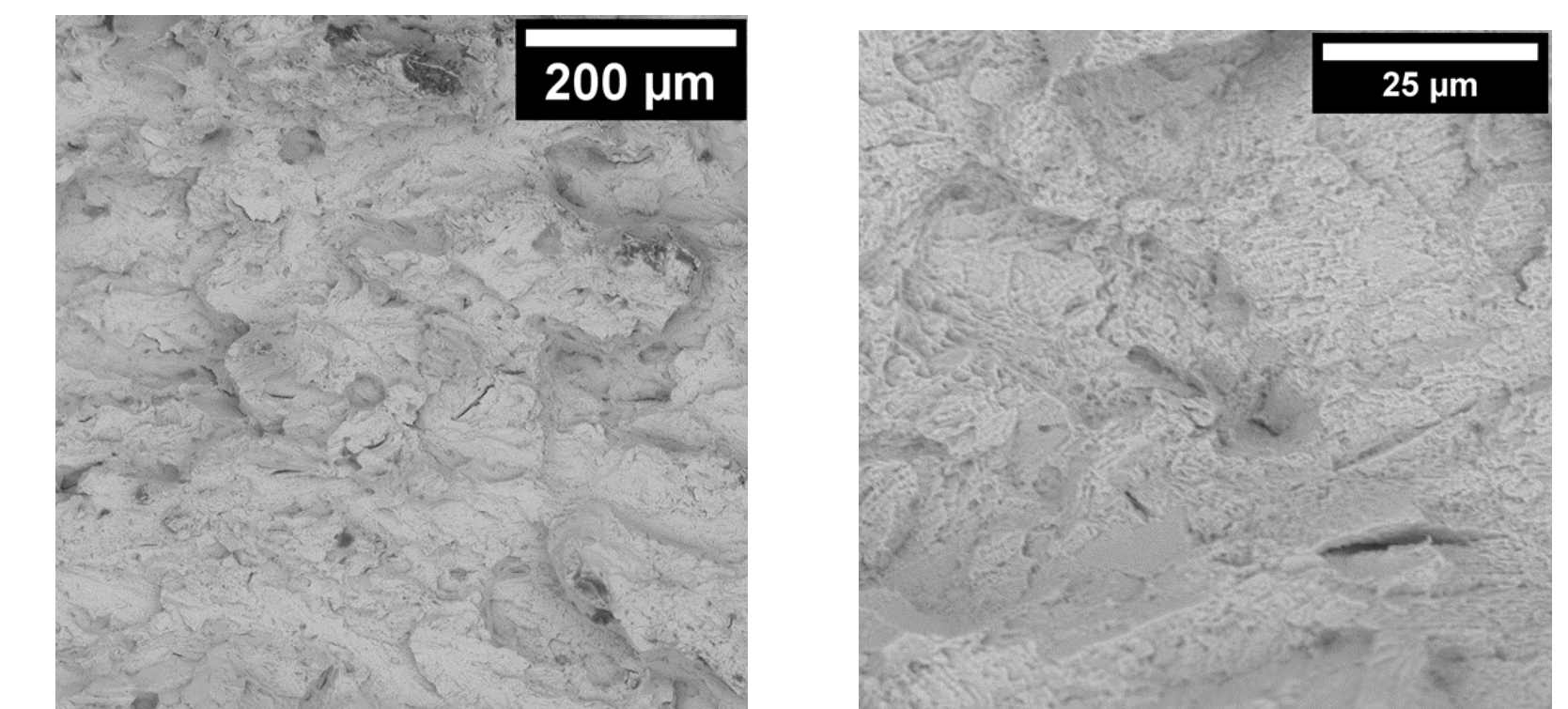
## Mechanical Analysis

### Tensile Testing

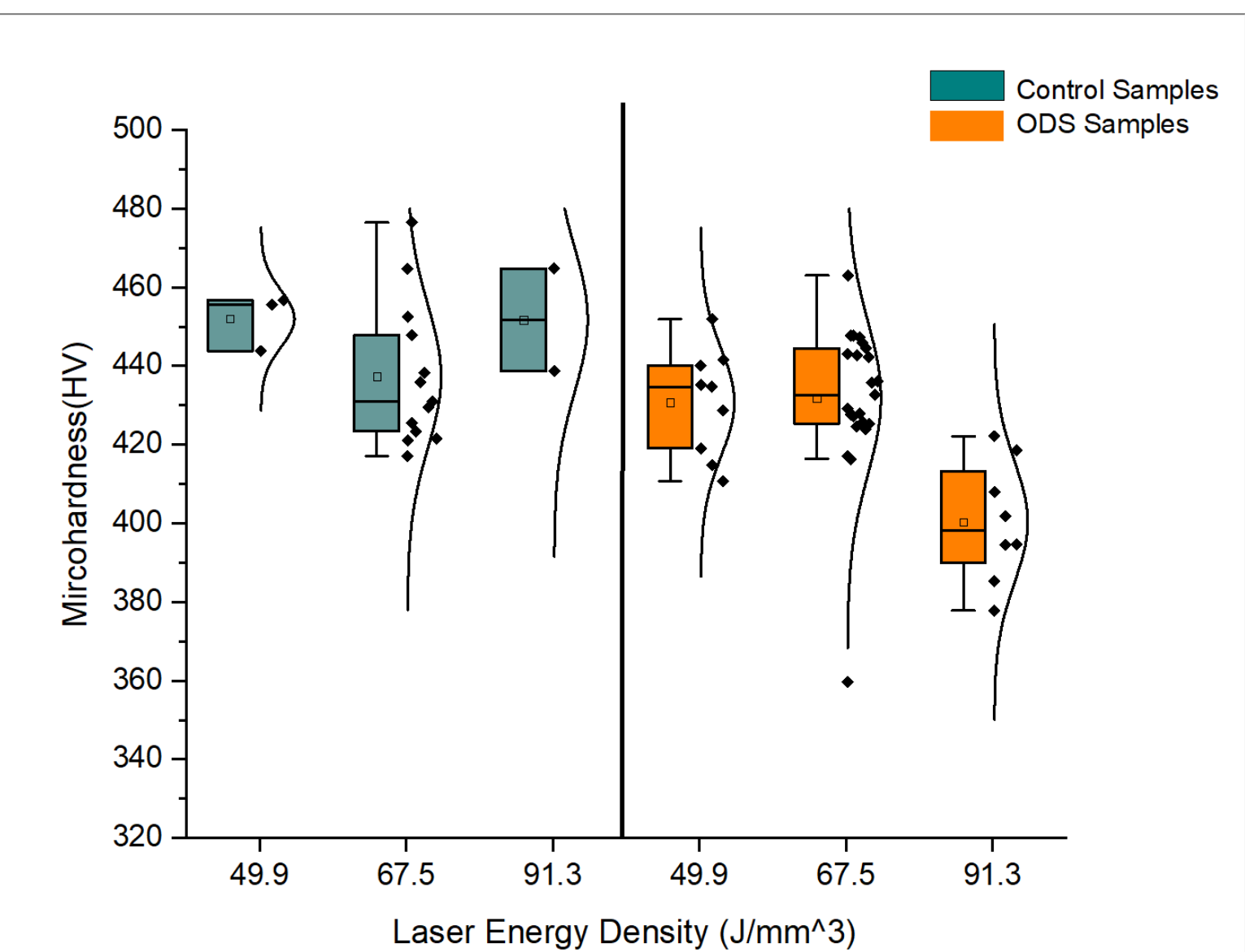


	Yield Strength (MPa)	Ultimate Tensile Strength (MPa)	Percent Elongation (%)	Young's Modulus (GPa)	Work Hardening Rate
Control E	878	1301	2.95	408	0.13
ODS C	797	1048	0.73	355	0.21
ODS E	756	971	0.42	413	0.24
ODS G	695	939	0.57	416	0.22

### SEM images of the ODS Tensile bar fracture surfaces



Control samples are 3 tensile tests represented by a single curve on this figure. Control samples displayed much higher ductility than ODS samples. While the ODS samples were predicted to have higher strengths, the control samples had higher strengths in these experiments. This is likely a result of agglomeration of the oxide particles and cracking in the Co-CrO samples. Sample ODS G was affected by surface defects during tensile testing. Fracture surfaces of the control and ODS after tensile testing both show cracking and nonductile fracture surfaces.



On this plot of microhardness versus laser energy density, the laser energy density of 49.9 J/mm³ corresponds to sample C, 91.3 J/mm³ to sample G, and 67.5 to samples A, E and I. The only notable influence of ODS is a decrease in microhardness at 91.3 J/mm³. Furthermore, energy density does not appear to have a major influence on the hardness of the sample. ODS samples show high variability in microhardness, which could be a result of the various microstructural features that were seen in microscopy.

## Conclusions and References

- Oxides agglomerates formed and caused cracking of the cobalt matrix
  - Control samples varied from dominant (111) or (200) planes, while ODS Samples always had dominant (111) planes
  - Tensile properties and microhardness usually decreased with the introduction of oxides
- Future Work**
- Investigate different powder mixing strategies to introduce oxides and prevent agglomeration.
  - Implement heat treatment to homogenize microstructure

### References

M. Brandt, "Powder bed fusion processes: An Overview", in *Laser Additive Manufacturing: Materials, design, technologies, and applications*. 2017  
 M. Cloots, et al. "Microstructural characteristics of the nickel-based alloy IN738LC and the cobalt-based alloy MAR-M509 produced by Selective Laser Melting," *Materials Science and Engineering* (2016).  
 Fragomeni, J., Deformation Pictures | *OrowanMechanisms*.

## Materials and Methods

Samples were produced through LPBF using the laser parameters listed below and the highlighted parameters were tested. For ODS, 1.75 wt% CrO powder was mixed with Mar-M509 powder. The XY and YZ planes of the samples were polished to 1 micron and then underwent vibratory polishing before analysis. No heat treatment was done on these samples.

Laser Power (W)	Laser Scan Speed (mm/s)		
	816	960	1104
242	A $\Psi=67.5$	B $\Psi=57.4$	C $\Psi=49.9$
285	D $\Psi=79.4$	E $\Psi=67.4$	F $\Psi=58.7$
328	G $\Psi=91.3$	H $\Psi=77.6$	I $\Psi=67.5$

XRD profiles were collected using a Bruker D8 focus instrument with a Cu ka-1 source with a scan time of 5 degrees/minute. SEM images of the characterization cubes and tensile bar fracture surfaces were taken on the quanta 650 and Nano science phenom

Tensile test were collected using a MTS Insight Electromechanical Testing system with displacement rate of 10mm/min. Microhardness tests were performed on the Leco Vickers Indenter with a load of 1kN for control samples and 300N for ODS samples. A 3x3 matrix of indents were performed, and average hardness were calculated. Densities were measured using Archimedes method. The cubic sample was immersed in DI water to measure a loss in weight equal to the weight of fluids it displaces.

Sample #	Measured Density (g/cm³):	Relative Density (%):	Porosity(%)
Sample A_ODS	8.662	97.766%	2.234%
Sample C_ODS	8.652	97.652%	2.348%
Sample E_ODS	8.674	97.903%	2.097%
Sample G_ODS	8.687	98.050%	1.950%
Sample I_ODS	8.648	97.608%	2.392%
Sample A_Control	8.705	98.255%	1.745%
Sample C_Control	8.772	99.001%	0.999%
Sample E_Control	8.784	99.146%	0.855%
Sample G_Control	8.769	98.969%	1.031%
Sample I_Control	8.777	99.058%	0.942%